$s_{1/2}$ and $p_{1/2}$ states to the cross section is at most a 10% contribution for the range of energies shown here.

Also in the experimental setup of Ref. 6 the efficiency of detecting the ^{5}Li* is a function of the relative energy [see Fig. 1(a)] and the method of calculating this efficiency is still open to question. This difficulty may be responsible for the difference between the peak positions of the calculation and experimental results.

In conclusion, whenever the ejectile state is unbound, the present method of calculating the energy dependence explicitly is appropriate and gives rather good agreement with the experimental results.

This work was supported in part by the U. S. Department of Energy.

[a]Present address: Department of Physics and Astrophysics, University of Colorado, Boulder, Colo. 80309.
[b]Present address: Department of Physics, University of Pittsburgh, Pittsburgh, Pa. 15261.
[c]Present address: Department of Physics, University of Pennsylvania, Philadelphia, Pa. 19104.

[1]G. J. Wozniak, D. P. Stahel, J. Cerny, and N. A. Jelley, Phys. Rev. C 14, 815 (1976); R. John, D. P. Stahel, G. J. Wozniak, J. Cerny, and H. P. Morsch, Phys. Lett. 65B, 339 (1976); D. Robson, Nucl. Phys. A204, 523 (1973); G. J. Wozniak, H. L. Harvey, K. H. Wilcox, and J. Cerny, Phys. Rev. Lett. 28, 1278 (1972).
[2]N. Austern, *Direct Nuclear Reactions* (Wiley-Interscience, New York, 1970).
[3]C. M. Vincent and H. T. Fortune, Phys. Rev. C 2, 782 (1970).
[4]N. Austern, *Direct Nuclear Reaction Theories* (Wiley-Interscience, New York, 1970), p. 78.
[5]L. Ray, W. R. Coker, and T. Udagawa, Phys. Lett. 56B, 318 (1975).
[6]A. Saha, R. Kamermans, J. van Driel, and H. P. Morsch, Phys. Lett. 79B, 363 (1978).
[7]P. D. Kunz, computer code DWUCK5 (unpublished).
[8]L. Brown, W. Haeberli, and W. Trächslin, Nucl. Phys. A90, 339 (1967); P. Schwandt, T. B. Clegg, and W. Haeberli, Nucl. Phys. A163, 432 (1971).
[9]N. J. Rybakov, V. A. Sidorov, and N. A. Vlasov, Nucl. Phys. 23, 491 (1961); J. Källne, B. Fagerström, O. Sundber, and G. Tibell, Phys. Lett. 52B, 313 (1974).

Maser Oscillation and Microwave Superradiance in Small Systems of Rydberg Atoms

M. Gross, P. Goy, C. Fabre, S. Haroche, and J. M. Raimond
Laboratoire de Physique de l'Ecole Normale Superieure, 75231 Paris Cedex 05, France
(Received 20 April 1979)

Superradiance and transient maser action have been obtained at millimeter wavelengths with alkali Rydberg atoms as the active medium. The emission was detected by monitoring the evolution of Rydberg-state populations using field ionization. Because of the strong Rydberg-atom–radiation-field coupling, the number of radiators at threshold is far smaller than in conventional masers. The estimated radiated energy is extremely low, 10 to 10^3 eV. Applications for spectroscopy and microwave detectors are considered.

Because of their unusually large electric-dipole matrix elements, Rydberg atoms interact very strongly with far-infrared or microwave radiation resonant on transitions connecting nearby levels. This feature explains the strong radio-emission by Rydberg states in the interstellar medium.[1] It also accounts for the extreme sensitivity of Rydberg atoms to microwave absorption,[2] for the superradiant cascade effects recently observed in Rydberg-atom fluorescence experiments,[3] and for radiative effects induced on these atoms by blackbody radiation.[4] We show in this Letter that these characteristics can also be exploited to develop "microscopic" coherent microwave sources which operate with a number of emitting atoms several orders of magnitude smaller than other atomic or molecular devices working at similar wavelengths. We report here on the operation of these new superradiant and maser systems, whose active medium is made of alkali-atom (Cs and Na) Rydberg states.[5] These devices, which behave as small single- or multiple-pass amplifiers of blackbody radiation, should provide new information about superradiance of small systems made of only a few atoms. More practically, they could become useful tools in spectroscopy or microwave detection technology.

Figure 1 shows the schemes of our Rydberg superradiant and maser systems [Figs. 1(a) and 1(b), respectively]. In both cases, a collimated atomic beam of alkali (10^{12} to 10^{14} atoms per second) is intersected at right angles by two pulsed, collinear, N_2-laser-pumped dye-laser beams

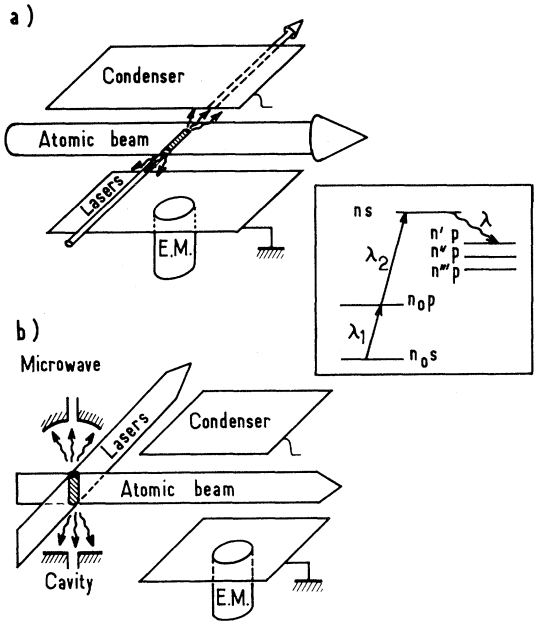

FIG. 1. (a) Sketch of microwave superradiant Rydberg system. (b) Sketch of Rydberg-state maser. Inset: Energy diagram showing relevant atomic levels.

(wavelengths λ_1 and λ_2). These beams excite the atoms from their n_0S ground state to the first resonant n_0P state ($\lambda_1 = 5890$ and 8523 Å for Na and Cs, respectively), then on to a Rydberg nS level ($n \sim 25$; $\lambda_2 = 4100$ and 5150 Å, respectively). This stepwise process is represented in the inset of Fig. 1. A pencil-shaped volume (length $L \sim 5$ mm, diameter $a \sim 1$ mm) of Rydberg atoms is thus prepared within about 2 ns. In the maser case [Fig. 1(b)], the active medium is pumped in a semiconfocal millimeter Fabry-Perot cavity (finesse $\mathfrak{F} \sim 200$ at $\lambda = 1.5$ mm), whose axis is perpendicular to the atomic and laser beams. The cavity length $l \sim 22$ mm is adjustable around focus.

Since populations are initially inverted on a large number of transitions connecting the pumped level to lower $n'P$ states (see inset in Fig. 1), such Rydberg systems could emit at many microwave or infrared wavelengths. Actually, superradiance occurs on the transition with the largest gain (i.e., lowest threshold). The threshold condition is expressed in terms of the population difference $N_{nn'}$ between nS and $n'P$ by the equation

$$N_{nn'} > \mu_{nn'}^{-1} \gamma_n \gamma_{nn'}^{-1}, \qquad (1)$$

where γ_n and $\gamma_{nn'}$ are the total emission rate from level ns and the partial rate on the $nS \rightarrow n'P$ transition, respectively, and

$$\mu_{nn'} = \frac{3}{8\pi} \frac{\lambda_{nn'}^2}{a^2} \sim \frac{3}{8\pi} \frac{\lambda_{nn'}}{L}$$

is a form factor depending on the transition wavelength $\lambda_{nn'}$ and on the shape of the active medium (whose Fresnel number $a^2/L\lambda_{nn'}$ is assumed to be of the order of unity.[6] Equation (1) shows that the system will superradiate on the transition with the largest $\mu_{nn'}\gamma_{nn'}$ factor, a condition which favors millimeter transitions towards nearby levels over shorter-wavelength ones. An estimation using a Coulomb approximation[7] shows indeed that $\gamma_{nn'}$ remains constant within a factor of 2 for all the $nS \rightarrow n'P$ transitions falling in the 1-mm–50-μm range, whereas $\mu_{nn'}$ strongly decreases when $\lambda_{nn'}$ is varied from the former to the latter value. Under the above conditions, both Na and Cs excited in nS levels ($n \sim 25$) will thus superradiate towards the $(n-1)P$ state, with $\lambda_{nn'}$ circa 1 mm.

In the maser [Fig. 1(b)], wavelength selection is, of course, helped by cavity tuning. The threshold is then given by a condition similar to Eq. (1) in which $\mu_{nn'}$ becomes a cavity filling factor and $N_{nn'}$ should be replaced by $\mathfrak{F}N_{nn'}$. Typical parameters for transitions around $n = 25$ are $\gamma_n \sim 10^5$ s^{-1}, $\gamma_{nn'} \sim 10^3$ s^{-1}, $\mu_{nn'} \sim 10^{-2}$. With these figures the inversion thresholds are $N_{nn'} \sim 10^5$ for superradiance and $N_{nn'} \sim 5 \times 10^2$ only for a maser with a $\mathfrak{F} \sim 200$ finesse.

It is interesting to compare these thresholds with those of other masers and superradiant systems operating at similar wavelengths. The ammonia beam maser ($\lambda \sim 12$ mm) works with typically 10^9 molecules in the cavity. The HF superradiant medium ($\lambda \sim 0.1$ mm) needs at least 10^{12} initially inverted molecules.[8] The huge difference in order of magnitude is due to the very large size of the transition matrix elements in the giant Rydberg atoms, which are typically of the order of 10^3 D for $n \sim 30$. As a consequence of their very small threshold, Rydberg masers or superradiant devices should have extremely low emitting power. Each atom yielding a photon of $\sim 10^{-3}$ eV, the expected total energy per pulse at threshold is only of about 1 eV for the maser and 10^2 eV for the superradiant case. The pulses lasting about 1 μs, expected peak powers are of the order of 10^{-13} and 10^{-11} W, respectively.

It is difficult to detect directly such small microwave bursts. In fact, the emitting atoms themselves can be made the detectors of their own emission by using the field-ionization detec-

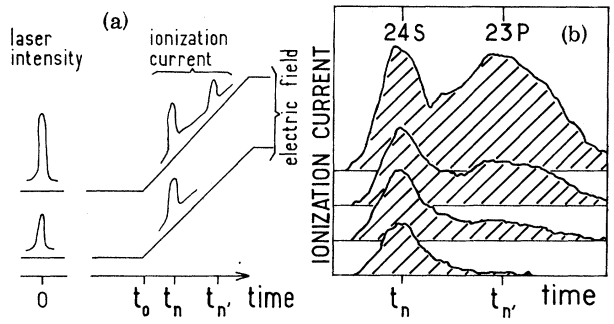

FIG. 2. (a) Schematics of the sequence of events experienced by active medium. Lower and upper traces correspond to situations below and above threshold, respectively. (b) Time-resolved ion-signal recordings showing superradiance on the $24S \rightarrow 23P$ transition in Cs (delay $t_0 = 2\ \mu s$). The four traces correspond, from bottom to top, to $N = 2\times10^5$, 4×10^5, 6×10^5, and 1.2×10^6. The time interval $t_{n'} - t_n$ is 60 ns.

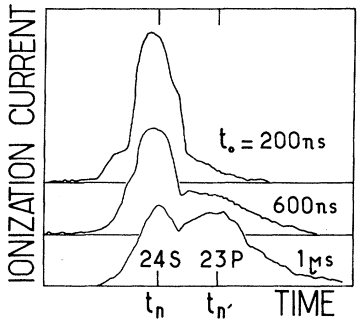

FIG. 3. Time-resolved ion-signal recordings exhibiting the evolution of the superradiant emission on the $24S \rightarrow 23P$ transition in Cs. The delay t_0 increases from the upper to the lower trace.

tion. The method[2] consists in applying at a given time an electric field F ionizing the Rydberg atoms. The ions are accelerated in the field and detected by an electron multiplier (EM in Fig. 1). The electric field is produced by the condenser plates represented in Figs 1(a) and 1(b). In the maser case, the detection occurs after the atoms have left the cavity. The principle of the procedure is sketched in Fig. 2(a) which shows the sequence of events experienced by the active medium below and above threshold (lower and upper traces, respectively). After laser excitation (time $t = 0$), the medium evolves until time t_0 when a ramp of electric field is applied. The field reaches at time t_n the value F_n corresponding to ionization of the initially pumped level. If the system is below threshold, a single ion signal should appear at time t_n [lower trace in Fig. 2(a)]. If, on the contrary, superradiance or maser action has taken place towards a lower $n'P$ level before t_0, atoms having decayed in this state will be ionized in a field $F_{n'}$ larger than F_n (because $n'P$ is a more tightly bound state than nS). A second ion signal should then appear at time $t_{n'} > t_n$ [upper trace in Fig. 2(a)]. The method has several attractive features: First, it is extremely sensitive. Single Rydberg atoms can be detected in each level which is equivalent to having a detector sensitive to single microwave photons. Second, it allows absolute calibration of the number of emitting atoms. The ion current is proportional to the number of ionized atoms in each level and the proportionality constant is estimated by reducing the pumping light intensity with calibrated filters until individual atom counts are registered. Finally, the method is highly selective. Each time-resolved peak can be assigned to a well-defined electric field threshold and to a given Rydberg state. Hence, this type of detection acts as a very sensitive microwave spectrometer.

The time-resolved ion signals are displayed on a fast transient digitizer (Tektronix 7912) and each event is registered by a tape recorder interfaced with the digitizer. We have recorded in this way a large number of superradiance signals on several $nS \rightarrow (n-1)P$ transitions in Cs.

Figure 2(b) shows four recordings of ionization signals following excitation of level $24S$ ($\lambda = 0.68$ mm). The delay t_0 is 2 μs. The four traces differ only by the laser pumping level, which increases from bottom to top. The threshold effect is clear: The population transfer to leve $23P$ appears only at high pumping intensities. Such recordings have shown that the threshold on this transition occurs for $N_{nn'} \sim 5\times10^5$, a figure in fair agreement with theory. The energy emitted in the pulses recorded in Fig. 2(b) is of the order of 5×10^2 eV only. By varying the delay t_0, one can record as a function of time the population difference $N_{nn'}$. Figure 3 shows, for the same transition, three signals corresponding to increasing t_0 values. The initial number of excited atoms is within ±5% the same in the three recordings ($N_{nn'} \sim 2\times10^6$). The increase with t_0 of the $23P$ ionization peak clearly shows that the emission process is delayed, as expected from a superradiant signal. The observed microsecond delay is much larger than the ones of former superradiant experiments performed at shorter wavelengths in less excited states of the alkalis.[9]

The operation of a Rydberg-state maser has

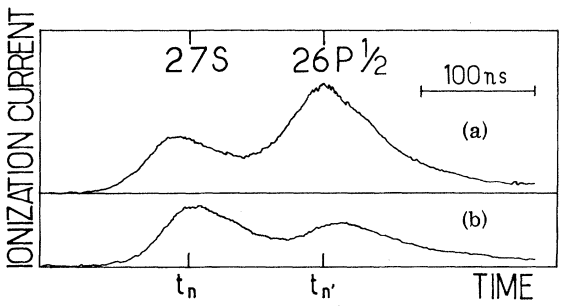

FIG. 4. Time-resolved Na ion-signal recordings averaged over 200 pulses, exhibiting maser effect. (a) The cavity is tuned on the $27S \rightarrow 26P_{1/2}$ transition. (b) The cavity is 40 Mhz off resonance (mirror separation l changed by 4 μm).

been achieved with the system sketched in Fig. 1(b), using a less dense beam of Na (about 10^4 excited atoms per pulse). Excitation and detection are the same as in the superradiance case with the only differences that the signals are now detected after a longer delay ($t_0 = 30$ μs) corresponding to the flight time of the atoms out of the cavity, and averaged over a few tens of laser pulses. Figure 4 shows the ionization signal following excitation of level $27S$ when the cavity is exactly tuned on the $27S \rightarrow 26P_{1/2}$ transition [Fig. 4(a)] and when it is slightly off resonance [40 Mhz detuning; Fig. 4(b)]. The emission wavelength is 1.49 mm. One clearly observes a cavity-enhanced transfer to the lower $26P_{1/2}$ level. (The small residual off-resonant transfer is probably due to spontaneous emission and a blackbody-radiation-induced transition[4]). Such maser effects have been observed for several $nS \rightarrow (n-1)P$ transitions ($25 < n < 35$). The estimated radiated energies per pulse are of the order of 10 eV. When the cavity length l, is swept, the maser signal appears around positions corresponding to different modes, separated by $\Delta l = \lambda/2$. For each mode, one observes two close resonant positions (separation $\delta l \ll \lambda/2$), corresponding to the P-state fine-structure splitting. From the δl measurement, we have deduced for the splittings of the $27P$, $28P$, and $33P$ levels, respectively, 314(30), 295(30), and 159(30) MHz. These results are in good agreement with the values 300(5), 266(4), and 161.5(1) MHz measured in a control microwave double-resonance experiment with use of the method described in Ref. 2.

Let us note that the long-wavelength superradiant and maser systems studied here are triggered by blackbody radiation rather than by spontaneous emission. They can thus be viewed as blackbody-radiation amplifiers. If the blackbody background is reduced by cooling, the same devices could, of course, be used to amplify any small microwave or far-infrared signal resonant on the atomic transition, thus enabling one to develop very sensitive new detectors in this wavelength domain. In the maser experiment, we have shown that the blackbody noise, selectively filtered by a cavity, can be used as a very simple, tunable, broadband microwave source for Rydberg-state spectroscopy. The resolution (30 MHz) is so far limited by the cavity finesse (200) and could be improved by several orders of magnitude. More fundamentally, we believe that these experiments open the way to the study of even smaller emitting systems (i.e., samples smaller than the atomic wavelength or with very small absolute atom number), a domain where there is still no comparison available between experiments and theory.

[1]B. Hoglund and P. G. Mezger, Science 150, 339 (1965).

[2]C. Fabre, S. Haroche, and P. Goy, Phys. Rev. A 18, 229 (1978).

[3]F. Gounand, M. Hugon, P. R. Fournier, and J. Berlande, J. Phys. B 12, 547 (1979).

[4]T. F. Gallagher and W. E. Cooke, Phys. Rev. Lett. 42, 835 (1979).

[5]While completing this manuscript, we learned of another unpublished experiment in which Rydberg-state superradiant signals have been observed [T. F. Gallagher and W. E. Cooke, Bull. Am. Phys. Soc. 23, 1103 (1978), and private communication].

[6]The atomic-beam transverse Doppler broadening is, in the microwave domain, smaller than γ_n. Hence, contrary to what happens in near-infrared superradiance, the Doppler dephasing time does not appear in the threshold condition.

[7]F. Gounand, to be published.

[8]N. Skribanowitz, I. P. Herman, J. C. McGillivray, and M. S.Feld, Phys. Rev. Lett. 30, 309 (1973).

[9]M. Gross, C. Fabre, P. Pillet, and S. Haroche, Phys. Rev. Lett. 36, 1035 (1976); H. M. Gibbs, Q. M. F. Vrehen, and H. M. J. Hikspoors, Phys. Rev. Lett. 39, 547 (1977).